CERN–TH/2003-026
hep-ph/0302104

The q_T spectrum of the Higgs boson at the LHC in QCD perturbation theory

G. Bozzi[(a,b)], **S. Catani**[(b,c)], **D. de Florian**[(d)*] **and M. Grazzini**[(a,b,c)]

[(a)]Dipartimento di Fisica, Università di Firenze, I-50019 Sesto Fiorentino, Florence, Italy
[(b)]INFN, Sezione di Firenze, I-50019 Sesto Fiorentino, Florence, Italy
[(c)]Theory Division, CERN, CH-1211 Geneva 23, Switzerland
[(d)]Departamento de Física, FCEYN, Universidad de Buenos Aires,
(1428) Pabellón 1 Ciudad Universitaria, Capital Federal, Argentina

Abstract

We consider the transverse-momentum (q_T) distribution of Higgs bosons produced at hadron colliders. We use a formalism that uniformly treats both the small-q_T and large-q_T regions in QCD perturbation theory. At small q_T ($q_T \ll M_H$, M_H being the mass of the Higgs boson), we implement an all-order resummation of logarithmically-enhanced contributions up to next-to-next-to-leading logarithmic accuracy. At large q_T ($q_T \gtrsim M_H$), we use fixed-order perturbation theory up to next-to-leading order. The resummed and fixed-order approaches are consistently matched by avoiding double-counting in the intermediate-q_T region. In this region, the introduction of unjustified higher-order terms is avoided by imposing unitarity constraints, so that the integral of the q_T spectrum exactly reproduces the perturbative result for the total cross section up to next-to-next-to-leading order. Numerical results at the LHC are presented. These show that the main features of the q_T distribution are quite stable with respect to perturbative QCD uncertainties.

CERN–TH/2003-026
February 2003

*Partially supported by Fundación Antorchas and CONICET.

The Standard Model (SM) of electroweak interactions has been spectacularly confirmed by experimental data. However the mechanism of mass generation remains to be understood. In its minimal version, the model predicts the existence of a scalar particle, the Higgs boson [1], as a vehicle of electroweak symmetry breaking, but this particle has so far eluded experimental discovery. The LEP collaborations have put a lower limit on the mass M_H of the SM Higgs boson at about 114 GeV [2], whereas fits to electroweak data prefer $M_H \lesssim 200$ GeV at 95% CL [3]. The next search for Higgs boson(s) will be carried out at hadron colliders, namely the Fermilab Tevatron [4] and the CERN LHC [5].

The main SM Higgs production mechanism at hadron colliders is the gluon fusion process. At leading order (LO), $\mathcal{O}(\alpha_{\rm S}^2)$, in the QCD coupling $\alpha_{\rm S}$ this process occurs through a heavy-quark (top-quark) loop and, being a gluon-initiated process, it is expected to receive large radiative corrections. It is thus important to perform an accurate evaluation of higher-order QCD contributions, together with a reliable estimate of the associated theoretical uncertainty.

The next-to-leading order (NLO) perturbative corrections to the total cross section for Higgs boson production via gluon fusion were computed in Refs. [6] (in the limit of an infinitely-heavy top quark) and [7] (including the dependence on the finite mass M_t of the top quark) and were found to be large (of the order of 80–100%), thus casting doubts upon the reliability of the perturbative expansion. In the last two years much effort has been devoted to improving the accuracy of the perturbative calculation. In the large-M_t limit, the next-to-next-to-leading order (NNLO) contribution has been computed in Ref. [8] and still higher-order contributions have been evaluated in Ref. [9] by implementing soft-gluon resummation. Since these beyond-NLO corrections are moderate, the perturbative QCD predictions for the total cross section are under good control now.

In this letter we consider a less inclusive observable, the transverse-momentum (q_T) distribution of the Higgs boson. An accurate theoretical prediction of this observable at the LHC [5] can be important to enhance the statistical significance of the signal over the background and to improve strategies for the extraction of the Higgs boson signal.

When studying the q_T distribution of the Higgs boson in QCD perturbation theory, it is convenient to start by considering separately the large-q_T and small-q_T regions. Roughly speaking, the large-q_T region is identified by the condition $q_T \gtrsim M_H$. In this region, the perturbative series is controlled by a small expansion parameter, $\alpha_{\rm S}(M_H^2)$, and calculations based on the truncation of the series at a fixed-order in $\alpha_{\rm S}$ are theoretically justified[†]. In the small-q_T region ($q_T \ll M_H$), where the bulk of events is produced, the convergence of the fixed-order expansion is spoiled, since the coefficients of the perturbative series in $\alpha_{\rm S}(M_H^2)$ are enhanced by powers of large logarithmic terms, $\ln^m(M_H^2/q_T^2)$. To obtain reliable perturbative predictions, these terms have to be systematically resummed to all orders in $\alpha_{\rm S}$ [11]. The fixed-order and resummed approaches have then to be consistently matched at intermediate values of q_T, so as to avoid the introduction of ad-hoc boundaries between the large-q_T and small-q_T regions.

Higgs boson production at large q_T has to be accompanied by the radiation of at least one recoiling parton, so the LO term for this observable is of $\mathcal{O}(\alpha_{\rm S}^3)$. The LO calculation was reported in Ref. [12]; it shows that the large-M_t approximation works well as long as both M_H and q_T are

[†]We are not considering the extreme limit $q_T \gg M_H$, where a resummation of enhanced perturbative terms is required [10].

smaller than M_t. Similar results on the validity of the large-M_t approximation were obtained in the case of the associated production of a Higgs boson plus 2 jets (2 recoiling partons at large transverse momenta) [13]. In the framework of the large-M_t approximation, the NLO QCD corrections to the transverse-momentum distribution of the Higgs boson were computed first numerically [14] and later analytically [15, 16]. In the large-q_T region, the overall effect of the NLO corrections to the q_T distribution is of the same size as that of the NLO corrections to the total cross section.

The method to systematically perform all-order resummation of logarithmically-enhanced terms at small q_T is known [11, 17–21] (see also the list of references in Sect. 5 of Ref. [22]). To correctly take into account the kinematics constraint of transverse-momentum conservation, the resummation procedure has to be carried out in b space, where the impact parameter b is the variable conjugate to q_T through a Fourier transformation. In the case of the Higgs boson, b-space resummation has been explicitly worked out at leading logarithmic (LL), next-to-leading logarithmic (NLL) [23, 24] and next-to-next-to-leading logarithmic (NNLL) [25] level. The q_T distribution is then obtained by performing the inverse Fourier (Bessel) transformation with respect to b. Various implementation formalisms [21, 26–31] have been proposed to transform the resummed expressions back to q_T space and to perform the matching with the fixed-order results at large q_T. Phenomenological applications to the Higgs boson q_T distribution have been presented in Refs. [32, 24, 33–37], by combining resummed and fixed-order perturbation theory at different levels of theoretical accuracy.

In the following we use the formalism described in Ref. [31] to compute the Higgs boson q_T distribution at the LHC. In particular, we combine the most advanced perturbative information that is available at present: NNLL resummation at small q_T and NLO calculations at large q_T. More details will be given elsewhere.

We consider the collision of two hadrons h_1 and h_2 with centre-of-mass energy $\sqrt{s}$. According to the QCD factorization theorem (see Ref. [38] and references therein), the transverse-momentum differential cross section for the production of the SM Higgs boson can be written as

$$\frac{d\sigma}{dq_T^2}(q_T, M_H, s) = \sum_{a,b} \int_0^1 dx_1 \int_0^1 dx_2 \, f_{a/h_1}(x_1, \mu_F^2) \, f_{b/h_2}(x_2, \mu_F^2) \, \frac{d\hat{\sigma}_{ab}}{dq_T^2}(q_T, M_H, \hat{s}; \alpha_S(\mu_R^2), \mu_R^2, \mu_F^2) \quad , \tag{1}$$

where $f_{a/h}(x, \mu_F^2)$ ($a = q, \bar{q}, g$) are the parton densities of the colliding hadrons at the factorization scale μ_F, $d\hat{\sigma}_{ab}/dq_T^2$ are the partonic cross sections, $\hat{s} = x_1 x_2 s$ is the partonic centre-of-mass energy, and μ_R is the renormalization scale. Throughout the paper we use parton densities as defined in the $\overline{\rm MS}$ factorization scheme, and $\alpha_S(q^2)$ is the QCD running coupling in the $\overline{\rm MS}$ renormalization scheme.

The partonic cross section is computable in QCD perturbation theory and, as discussed above, it is evaluated by introducing the decomposition

$$\frac{d\hat{\sigma}_{ab}}{dq_T^2} = \frac{d\hat{\sigma}_{ab}^{(\rm res.)}}{dq_T^2} + \frac{d\hat{\sigma}_{ab}^{(\rm fin.)}}{dq_T^2} \, . \tag{2}$$

The first term on the right-hand side contains all the logarithmically-enhanced contributions, $\alpha_S^n/q_T^2 \, \ln^m Q^2/q_T^2$, at small q_T, and has to be evaluated by resumming them to all orders in α_S. The second term is free of such contributions, and can be computed by fixed-order truncation of the perturbative series.

The resummed component $d\hat{\sigma}_{ac}^{(\mathrm{res.})}$ of the partonic cross section is written as

$$\frac{d\hat{\sigma}_{ac}^{(\mathrm{res.})}}{dq_T^2}(q_T, M_H, \hat{s}; \alpha_{\mathrm{S}}(\mu_R^2), \mu_R^2, \mu_F^2) = \frac{1}{2}\int_0^\infty db\; b\; J_0(bq_T)\; \mathcal{W}_{ac}(b, M_H, \hat{s}; \alpha_{\mathrm{S}}(\mu_R^2), \mu_R^2, \mu_F^2)\;, \qquad (3)$$

where $J_0(x)$ is the 0th-order Bessel function. The factor $\mathcal{W}$ embodies the all-order dependence on the large logarithms $L = \ln M_H^2 b^2$ at large b, which corresponds to the q_T-space terms $\ln M_H^2/q_T^2$ that are logarithmically enhanced at small q_T (the limit $q_T \ll M_H$ corresponds to $M_H b \gg 1$, because b is the variable conjugate to q_T). Resummation of these large logarithms is better expressed by defining the N-moments $\mathcal{W}_N$ of $\mathcal{W}$ with respect to $z = M_H^2/\hat{s}$ at fixed M_H:

$$\mathcal{W}_{ac,\,N}(b, M_H; \alpha_{\mathrm{S}}(\mu_R^2), \mu_R^2, \mu_F^2) \equiv \int_0^1 dz\; z^{N-1}\; \mathcal{W}_{ac}(b, M_H, \hat{s} = M_H^2/z; \alpha_{\mathrm{S}}(\mu_R^2), \mu_R^2, \mu_F^2)\;. \qquad (4)$$

The resummation structure of $\mathcal{W}_{ac,\,N}$ can indeed be organized in exponential form as follows:

$$\begin{aligned}\mathcal{W}_N(b, M_H; \alpha_{\mathrm{S}}(\mu_R^2), \mu_R^2, \mu_F^2) &= \mathcal{H}_N\left(\alpha_{\mathrm{S}}(\mu_R^2); M_H^2/\mu_R^2, M_H^2/\mu_F^2\right) \\ &\quad \times \exp\{\mathcal{G}_N(\alpha_{\mathrm{S}}(\mu_R^2), bM_H; M_H^2/\mu_R^2, M_H^2/\mu_F^2)\}\;\;, \end{aligned} \qquad (5)$$

where the subscripts denoting the flavour indices are understood[‡].

All the large logarithmic terms $\alpha_{\mathrm{S}}^n L^m = \alpha_{\mathrm{S}}^n \ln^m M_H b$ with $1 \le m \le 2n$ are included (actually, the complete dependence on b is included) in the form factor $\exp\{\mathcal{G}\}$. More importantly, all the logarithmic contributions to $\mathcal{G}$ with $n+2 \le m \le 2n$ are vanishing. Thus, the exponent $\mathcal{G}$ can systematically be expanded as

$$\begin{aligned}\mathcal{G}_N(\alpha_{\mathrm{S}}, bM_H; M_H^2/\mu_R^2, M_H^2/\mu_F^2) &= \widetilde{L}\, g^{(1)}(\alpha_{\mathrm{S}}\widetilde{L}) + g_N^{(2)}(\alpha_{\mathrm{S}}\widetilde{L}; M_H^2/\mu_R^2) \\ &\quad + \alpha_{\mathrm{S}}\, g_N^{(3)}(\alpha_{\mathrm{S}}\widetilde{L}; M_H^2/\mu_R^2, M_H^2/\mu_F^2) + \ldots\;\;, \end{aligned} \qquad (6)$$

where $\alpha_{\mathrm{S}} = \alpha_{\mathrm{S}}(\mu_R^2)$ and the functions $g^{(n)}(\alpha_{\mathrm{S}}\widetilde{L})$ are defined such that $g^{(n)} = 0$ when $\alpha_{\mathrm{S}}\widetilde{L} = 0$. Thus the term $\widetilde{L}g^{(1)}$ collects the LL contributions $\alpha_{\mathrm{S}}^n \widetilde{L}^{n+1}$; the function $g^{(2)}$ resums the NLL contributions $\alpha_{\mathrm{S}}^n \widetilde{L}^n$; $g^{(3)}$ controls the NNLL terms $\alpha_{\mathrm{S}}^n \widetilde{L}^{n-1}$, and so forth. Note that in the expansion (6) the logarithmic variable L has been replaced by

$$\widetilde{L} = \ln\left(M_H^2 b^2/b_0^2 + 1\right)\;\;, \qquad (7)$$

where $b_0 = 2e^{-\gamma}$. In the resummation region $M_H b \gg 1$, the replacement is fully legitimate since $\widetilde{L} \sim L$. The reason for using $\widetilde{L}$ rather than L is discussed below.

The function $\mathcal{H}_N$ in Eq. (5) does not depend on b and, hence, its evaluation does not require resummation of large logarithmic terms. It can be expanded in powers of $\alpha_{\mathrm{S}} = \alpha_{\mathrm{S}}(\mu_R^2)$ as

$$\begin{aligned}\mathcal{H}_N(\alpha_{\mathrm{S}}; M_H^2/\mu_R^2, M_H^2/\mu_F^2) &= \sigma_0\; \alpha_{\mathrm{S}}^2\Big[1 + \frac{\alpha_{\mathrm{S}}}{2\pi}\,\mathcal{H}_N^{(1)}(M_H^2/\mu_R^2, M_H^2/\mu_F^2) \\ &\quad + \left(\frac{\alpha_{\mathrm{S}}}{2\pi}\right)^2 \mathcal{H}_N^{(2)}(M_H^2/\mu_R^2, M_H^2/\mu_F^2) + \ldots\Big]\;\;, \end{aligned} \qquad (8)$$

[‡]More precisely, we are presenting the resummation formulae in a simplified form which is valid when there is a single species of partons. In general, the exponential is replaced by an exponential matrix with respect to the flavour indices of the partons.

where $\sigma_0 = G_F/(288\pi\sqrt{2})$ is the Born level cross section in the large-M_t approximation, and $G_F = 1.16639 \times 10^{-5}\,\mathrm{GeV}^{-2}$ is the Fermi constant.

The 'finite' component $d\hat{\sigma}_{ab}^{(\mathrm{fin.})}$ of the partonic cross section does not require resummation of large logarithmic terms either. We compute it as follows:

$$\frac{d\hat{\sigma}_{ab}^{(\mathrm{fin.})}}{dq_T^2} = \left[\frac{d\hat{\sigma}_{ab}}{dq_T^2}\right]_{\mathrm{f.o.}} - \left[\frac{d\hat{\sigma}_{ab}^{(\mathrm{res.})}}{dq_T^2}\right]_{\mathrm{f.o.}}. \tag{9}$$

The first term on the right-hand side is the usual perturbative series for the partonic cross section truncated at a given fixed order in α_{S}. The second term is obtained by truncating the resummed component in Eq. (3) at the *same* fixed order in α_{S}. The (small-q_T) resummed and (large-q_T) fixed-order approaches are thus consistently matched by avoiding double-counting in the intermediate-q_T region. This procedure guarantees that the right-hand side of Eq. (2) contains the full information of the perturbative calculation up to the fixed order specified by Eq. (3) plus resummation of logarithmically-enhanced contributions from higher orders.

A few distinctive features of the formalism described so far require some comments.

We implement perturbative QCD resummation at the level of the partonic cross section. In the factorization formula (1), the parton densities are thus evaluated at the factorization scale μ_F, as in the customary perturbative calculations at large q_T. The central value of μ_F and μ_R has to be set equal to M_H, the typical hard scale of the process, and the theoretical accuracy of the resummed calculation can be investigated as in fixed-order calculations, by varying μ_F and μ_R around this central value.

The variables L and $\widetilde{L}$ are equivalent to organize the resummation formalism in the region $M_H b \gg 1$. The use of the variable $\widetilde{L}$ is inspired by the procedure introduced in Ref. [39] to deal with kinematical constraints when performing soft-gluon resummation in e^+e^- event shapes. When $M_H b \ll 1$, $\widetilde{L} \to 0$ and $\exp\{\mathcal{G}\} \to 1$. Therefore, using the definition in Eq. (7), we avoid the introduction of all-order contributions in the small-b region, where the use of the large-b resummation formalism is not justified. In particular, $\exp\{\mathcal{G}\} = 1$ at $b = 0$. This implies that the integral over q_T of $d\sigma/dq_T$ exactly reproduces the fixed-order calculation of the total cross section. Note that the bulk of the q_T distribution is in the region $q_T \lesssim M_H$. Since resummed and fixed-order perturbation theory controls the small-q_T and large-q_T regions respectively, the total cross section constraint mainly acts on the size of the higher-order contributions introduced in the intermediate-q_T region by the matching procedure.

It is known [26–28, 40, 41] that non-perturbative effects have an increasing role in the q_T distribution as q_T decreases. However, we do not include non-perturbative contributions. The main goal of the quantitative study presented below is to investigate the predictivity of QCD within a purely perturbative framework. In particular, we want to examine how the Higgs boson q_T distribution is affected by perturbative QCD uncertainties, such as its dependence on scale variations and on higher-order contributions.

The functions $g_N^{(k)}(\alpha_{\mathrm{S}}\widetilde{L})$ and the coefficients $\mathcal{H}_N^{(k)}$ in Eqs. (6) and (8) can be expressed (see for instance Ref. [29]) in terms of perturbative coefficients known as $A^{(n)}$, $B^{(n)}$, $C^{(n)}$ [21] and $H^{(n)}$ [31]. In particular, $g^{(1)}$ depends on $A^{(1)}$, $g_N^{(2)}$ also depends on $B^{(1)}$ and $A^{(2)}$ [23], $g_N^{(3)}$ also depends on $H^{(1)}$, $C^{(1)}$ [24], $B^{(2)}$ [25,16] and $A^{(3)}$, $\mathcal{H}_N^{(1)}$ depends on $H^{(1)}$ and $C^{(1)}$, $\mathcal{H}_N^{(2)}$ also depends on $H^{(2)}$ and

$C^{(2)}$. We also observe that the functions $g_N^{(2)}$ and $g_N^{(3)}$ receive additional contributions respectively from the LO and NLO anomalous dimensions that control the evolution of the parton densities. The NNLL coefficient $A^{(3)}$ is not yet known. In the following we assume that its value is the same as the one [42] that appears in resummed calculations of soft-gluon contributions near threshold. The coefficient $\mathcal{H}_N^{(2)}$ is not known in analytic form either. However, within our formalism we can exploit the property that the integral of the q_T distribution exactly matches the fixed-order calculation of the total cross section. From the known NNLO result for the total cross section [8], we thus extract $\mathcal{H}_N^{(2)}$ in (approximate) numerical form. As pointed out in Ref. [31], the coefficients $B^{(n)}$, $C^{(n)}$ and $H^{(n)}$ cannot separately be defined without fixing a resummation scheme. Note, however, that the dependence on the choice of the resummation scheme cancels by recasting the resummed formulae in the form of Eq. (5): the functions $g_N^{(k)}(\alpha_{\rm S}\widetilde{L})$ and the coefficients $\mathcal{H}_N^{(k)}$in Eqs. (6) and (8) are explicitly resummation-scheme independent.

The functions $g_N^{(k)}(\alpha_{\rm S}\widetilde{L})$ are singular when $\lambda = \beta_0\alpha_{\rm S}\widetilde{L} \to 1$ (β_0 is the first coefficient of the QCD β-function). The singular behaviour is related to the presence of the Landau pole in the perturbative running of the QCD coupling $\alpha_{\rm S}(q^2)$. To properly define the b integration in Eq. (3), a prescription to deal with these singularities has to be introduced. Here we follow Ref. [43] and deform the integration contour in the complex b space, as an extension of the minimal prescription of Ref. [44].

In the following we present quantitative results at NLL+LO and NNLL+NLO accuracy. We implement Eqs. (2) and (9). At NLL+LO accuracy, we compute $d\sigma^{(\rm res.)}$ at NLL accuracy (we include the coefficient $\mathcal{H}_N^{(1)}$ and the functions $g_N^{(1)}$ and $g_N^{(2)}$), and we match it with $[d\sigma]_{\rm f.o.}$ evaluated at LO (i.e. at $\mathcal{O}(\alpha_{\rm S}^3)$). At NNLL+NLO accuracy, we also include $\mathcal{H}_N^{(2)}$ and $g_N^{(3)}$ in the resummed component and we evaluate $[d\sigma]_{\rm f.o.}$ at NLO (i.e. at $\mathcal{O}(\alpha_{\rm S}^4)$). As for the evaluation of $[d\sigma]_{\rm f.o.}$, we use the Monte Carlo program of Ref. [14]. The numerical results are obtained by using the MRST2001 set of parton distributions [45] and choosing $M_H = 125$ GeV. At NLL+LO we use LO parton densities and 1-loop $\alpha_{\rm S}$, whereas at NNLL+NLO we use NLO parton densities and 2-loop $\alpha_{\rm S}$.

The NLL+LO results at the LHC are shown in Fig. 1. In the left-hand side, the full NLL+LO result (solid line) is compared with the LO one (dashed line) at the default scales $\mu_F = \mu_R = M_H$. We see that the LO calculation diverges to $+\infty$ as $q_T \to 0$. The effect of the resummation is relevant below $q_T \sim 100$ GeV. In the right-hand side we show the NLL+LO band that is obtained by varying $\mu_F = \mu_R$ between $1/2M_H$ and $2M_H$. The scale dependence increases from about $\pm 10\%$ at the peak to about $\pm 20\%$ at $q_T = 100$ GeV. The integral of the resummed curve is in good agreement with the value of the NLO total cross section evaluated with LO parton densities and 1-loop $\alpha_{\rm S}$, the small difference being due to the (improvable) numerical precision of our code.

The NNLL+NLO results at the LHC are shown in Fig. 2. In the left-hand side, the full result (solid line) is compared with the NLO one (dashed line) at the default scales $\mu_F = \mu_R = M_H$. The NLO result diverges to $-\infty$ as $q_T \to 0$ and, at small values of q_T, it has an unphysical peak (the top of the peak is above the vertical scale of the plot) which is produced by the numerical compensation of negative leading logarithmic and positive subleading logarithmic contributions. It is interesting to compare the LO and NLL+LO curves in Fig. 1 and the NLO curve in Fig. 2. At $q_T \sim 50$ GeV, the q_T distribution sizeably increases when going from LO to NLO and from NLO to NLL+LO. This implies that in the intermediate-q_T region there are important contributions

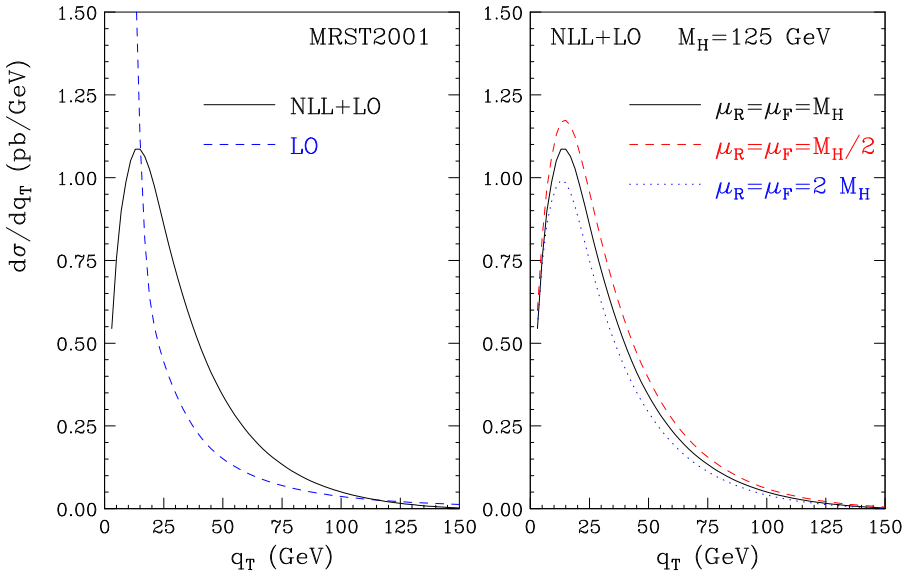

Figure 1: *LHC results at NLL+LO accuracy.*

that have to be resummed to all orders rather than simply evaluated at the next perturbative order. The q_T distribution is (moderately) harder at NNLL+NLO than at NLL+LO accuracy. The height of the NNLL peak is a bit lower than the NLL one. This is mainly due to the fact that the total NNLO cross section (computed with NLO parton densities and 2-loop α_S), which fixes the value of the q_T integral of our resummed result, is slightly smaller than the NLO one, whereas the high-q_T tail is higher at NNLL order, thus leading to a reduction of the cross section at small q_T. We find that the contribution of $A^{(3)}$ (recall that we are using an educated guess on the value of the coefficient $A^{(3)}$) can safely be neglected. The coefficient $\mathcal{H}_N^{(2)}$ contributes significantly, and enhances the q_T distribution by roughly 20% in the region of intermediate and small values of q_T. The resummation effect starts to be visible below $q_T \sim 100$ GeV, and it increases the NLO result by about 40% at $q_T = 50$ GeV. The right-hand side of Fig. 2 shows the scale dependence computed as in Fig. 1. The scale dependence is now about $\pm 6\%$ at the peak and increases to $\pm 20\%$ at $q_T = 100$ GeV. Comparing Figs. 1 and 2, we see that the NNLL+NLO band is smaller than the NLL+LO one and overlaps with the latter at $q_T \lesssim 100$ GeV. This suggests a good convergence of the resummed perturbative expansion.

We have considered perturbative QCD predictions for the Higgs boson q_T distribution at the LHC. We have shown that the main features of the q_T distribution are quite stable with respect to perturbative uncertainties (scale variations, inclusion of higher orders in the resummed expansion). More details about the formalism and our numerical results will be presented in a future publication, where we shall also consider the inclusion of non-perturbative contributions. Available studies [35–37] of non-perturbative contributions at the LHC estimate effects (at most) of the order of a few per cent when $q_T \gtrsim 10$ GeV. These effects are smaller than the resummation effects examined here.

Acknowledgements

We would like to thank Werner Vogelsang for discussions. S.C. wishes to thank Luca Trentadue for their early collaboration on Higgs boson production in hadronic collisions.

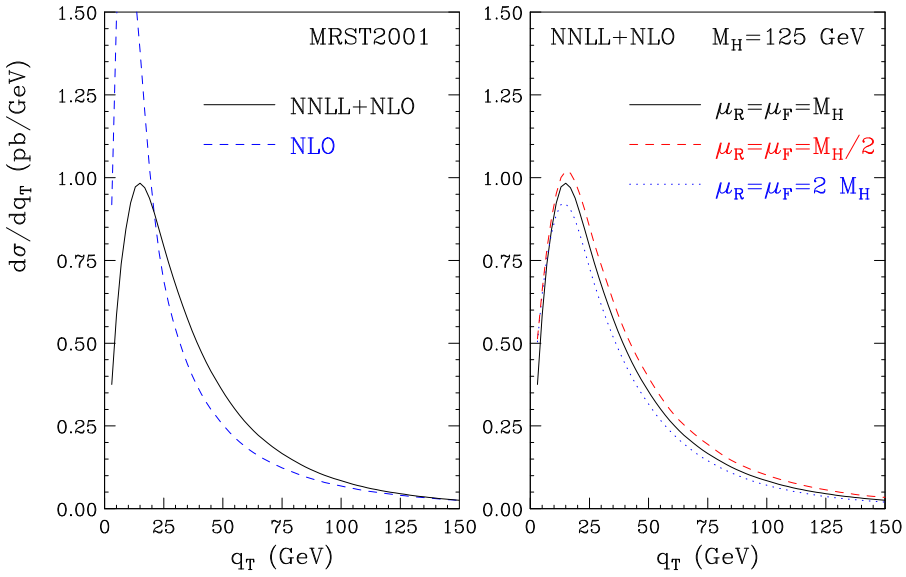

Figure 2: *LHC results at NNLL+NLO accuracy.*

References

1. For a review on Higgs physics in and beyond the Standard Model, see J. F. Gunion, H. E. Haber, G. L. Kane and S. Dawson, *The Higgs Hunter's Guide* (Addison-Wesley, Reading, Mass., 1990); M. Carena and H. E. Haber, preprint FERMILAB-PUB-02-114-T [hep-ph/0208209].

2. A. Heister *et al.* [ALEPH Collaboration], Phys. Lett. B **526** (2002) 191; P. Abreu *et al.* [DELPHI Collaboration], Phys. Lett. B **499** (2001) 23; P. Achard *et al.* [L3 Collaboration], Phys. Lett. B **517** (2001) 319; G. Abbiendi *et al.* [OPAL Collaboration], hep-ex/0209078.

3. The LEP Collaborations, the LEP Electroweak Working Group and the SLD Heavy Flavour Group, report LEPEWWG/2002–02, hep-ex/0212036.

4. M. Carena *et al.*, *Report of the Tevatron Higgs working group*, hep-ph/0010338.

5. CMS Coll., *Technical Proposal*, report CERN/LHCC/94-38 (1994); ATLAS Coll., *ATLAS Detector and Physics Performance: Technical Design Report*, Vol. 2, report CERN/LHCC/99-15 (1999).

6. S. Dawson, Nucl. Phys. B **359** (1991) 283; A. Djouadi, M. Spira and P. M. Zerwas, Phys. Lett. B **264** (1991) 440.

7. M. Spira, A. Djouadi, D. Graudenz and P. M. Zerwas, Nucl. Phys. B **453** (1995) 17.

8. S. Catani, D. de Florian and M. Grazzini, JHEP **0105** (2001) 025; R. V. Harlander and W. B. Kilgore, Phys. Rev. D **64** (2001) 013015, Phys. Rev. Lett. **88** (2002) 201801; C. Anastasiou and K. Melnikov, Nucl. Phys. B **646** (2002) 220.

9. S. Catani, D. de Florian, M. Grazzini and P. Nason, in W. Giele *et al.*, hep-ph/0204316, p. 51, contributed to the Les Houches 2001 Workshop on *Physics at TeV Colliders*.

10. E. L. Berger, J. w. Qiu and X. f. Zhang, Phys. Rev. D **65** (2002) 034006.

11. Y. L. Dokshitzer, D. Diakonov and S. I. Troian, Phys. Rep. **58** (1980) 269.

12. R. K. Ellis, I. Hinchliffe, M. Soldate and J. J. van der Bij, Nucl. Phys. B **297** (1988) 221; U. Baur and E. W. Glover, Nucl. Phys. B **339** (1990) 38.

13. V. Del Duca, W. Kilgore, C. Oleari, C. Schmidt and D. Zeppenfeld, Nucl. Phys. B **616** (2001) 367.

14. D. de Florian, M. Grazzini and Z. Kunszt, Phys. Rev. Lett. **82** (1999) 5209.

15. V. Ravindran, J. Smith and W. L. Van Neerven, Nucl. Phys. B **634** (2002) 247.

16. C. J. Glosser and C. R. Schmidt, JHEP **0212** (2002) 016.

17. G. Parisi and R. Petronzio, Nucl. Phys. B **154** (1979) 427.

18. G. Curci, M. Greco and Y. Srivastava, Nucl. Phys. B **159** (1979) 451.

19. J. C. Collins and D. E. Soper, Nucl. Phys. B **193** (1981) 381 [Erratum-ibid. B **213** (1983) 545].

20. J. Kodaira and L. Trentadue, Phys. Lett. B **112** (1982) 66, report SLAC-PUB-2934 (1982).

21. J. C. Collins, D. E. Soper and G. Sterman, Nucl. Phys. B **250** (1985) 199.

22. S. Catani et al., hep-ph/0005025, in the Proceedings of the CERN Workshop on *Standard Model Physics (and more) at the LHC*, eds. G. Altarelli and M.L. Mangano (CERN 2000-04, Geneva, 2000), p. 1.

23. S. Catani, E. D'Emilio and L. Trentadue, Phys. Lett. B **211** (1988) 335.

24. R. P. Kauffman, Phys. Rev. D **45** (1992) 1512.

25. D. de Florian and M. Grazzini, Phys. Rev. Lett. **85** (2000) 4678, Nucl. Phys. B **616** (2001) 247.

26. J. C. Collins and D. E. Soper, Nucl. Phys. B **197** (1982) 446.

27. G. Altarelli, R. K. Ellis, M. Greco and G. Martinelli, Nucl. Phys. B **246** (1984) 12.

28. R. K. Ellis and S. Veseli, Nucl. Phys. B **511** (1998) 649.

29. S. Frixione, P. Nason and G. Ridolfi, Nucl. Phys. B **542** (1999) 311.

30. A. Kulesza and W. J. Stirling, Nucl. Phys. B **555** (1999) 279, JHEP **0001** (2000) 016.

31. S. Catani, D. de Florian and M. Grazzini, Nucl. Phys. B **596** (2001) 299.

32. I. Hinchliffe and S. F. Novaes, Phys. Rev. D **38** (1988) 3475.

33. R. P. Kauffman, Phys. Rev. D **44** (1991) 1415.

34. C. P. Yuan, Phys. Lett. B **283** (1992) 395.

35. C. Balazs and C. P. Yuan, Phys. Lett. B **478** (2000) 192.

36. C. Balazs, J. Huston and I. Puljak, Phys. Rev. D **63** (2001) 014021; see also Sect. 5.4 in W. Giele *et al.*, hep-ph/0204316, contributed to the Les Houches 2001 Workshop on *Physics at TeV Colliders*.

37. E. L. Berger and J. w. Qiu, preprint ANL-HEP-PR-02-057 [hep-ph/0210135].

38. J. C. Collins, D. E. Soper and G. Sterman, in *Perturbative Quantum Chromodynamics*, ed. A.H. Mueller (World Scientific, Singapore, 1989), p. 1.

39. S. Catani, L. Trentadue, G. Turnock and B. R. Webber, Nucl. Phys. B **407** (1993) 3.

40. A. Guffanti and G. E. Smye, JHEP **0010** (2000) 025.

41. J. w. Qiu and X. f. Zhang, Phys. Rev. Lett. **86** (2001) 2724, Phys. Rev. D **63** (2001) 114011.

42. A. Vogt, Phys. Lett. B **497** (2001) 228; C. F. Berger, Phys. Rev. D **66** (2002) 116002.

43. E. Laenen, G. Sterman and W. Vogelsang, Phys. Rev. Lett. **84** (2000) 4296; A. Kulesza, G. Sterman and W. Vogelsang, Phys. Rev. D **66** (2002) 014011.

44. S. Catani, M. L. Mangano, P. Nason and L. Trentadue, Nucl. Phys. B **478** (1996) 273.

45. A. D. Martin, R. G. Roberts, W. J. Stirling and R. S. Thorne, Eur. Phys. J. C **23** (2002) 73.